Direct Evidence of Nanometric Invasionlike Grain Boundary Penetration in the Al/Ga System

E. Pereiro-López,[1] W. Ludwig,[1,2,*] D. Bellet,[3] P. Cloetens,[1] and C. Lemaignan[3,4]

[1]*European Synchrotron Radiation Facility, BP 220, 38043 Grenoble, France*

[2]*Groupe d'Etude de Métallurgie Physique et de Physique des Matériaux, INSA de Lyon, 69621 Villeurbanne Cedex, France*

[3]*Laboratoire Génie Physique et Mécanique des Matériaux, ENSPG, BP 46, 38 400 Saint-Martin-d'Hères Cedex, France*

[4]*CEA DEC-Dir, CEA Grenoble, 38041 Grenoble, France*

(Received 14 July 2005; published 14 November 2005)

We report the first *in situ* results of deformation during grain boundary penetration in the Al/Ga system, obtained with a novel, nondestructive hard x-ray synchrotron projection microscopy technique. Focusing the beam to a state-of-the-art spot size of 90×90 nm^2, we demonstrate that penetration is accompanied by continuous relative separation of the Al grains of the same final amplitude as the final Ga layer thickness in the absence of external stress. The formation of nanometric intergranular liquid layers is originated by a crack propagation process and inherently implies the presence of weak stress levels.

DOI: 10.1103/PhysRevLett.95.215501 PACS numbers: 62.20.Mk, 07.85.Tt

Introduction.—Liquid metal embrittlement (LME) is a well documented, but still poorly understood, failure mechanism [1] which may lead to brittle, intergranular failure of normally ductile metals and alloys when stressed while in contact with a liquid metal. The complexity of the phenomenon associated with the experimental difficulties [the nonequilibrium nature of the grain boundary penetration (GBP), fast crack growth rates, and nonadaptability of many experimental techniques] has inhibited the understanding of the interplay of the dynamic processes involved [2]. Recent experimental and theoretical work clearly demonstrates that segregation of less than one monolayer of Bi atoms can lead to significant changes in the electronic structure, thereby provoking embrittlement of grain boundaries (GBs) in Cu bicrystals [3]. There is evidence that a similar mechanism is responsible for GB brittleness in the Al/Ga system [4]. However, it is still unclear how far embrittlement at the atomistic level relates to the spectacular and intriguing process of GBP in the Al/Ga system, where the penetration of liquid Ga leads to the formation of up to several hundred nanometers thick wetting layers in the absence of any applied load [5–7].

A variety of models [8–13] has been proposed to explain the establishment of such microscopic wetting layers, but none of them can fully account for the different aspects of the experimental observations. One can roughly divide these models in two main groups: (1) GBP would basically be a replacement of solid metal atoms by liquid metal atoms, where the volume required to accommodate the liquid layer would be created via liquid phase diffusion mass transport of solid metal towards the external sample surfaces; (2) GBP would be an invasionlike process for which the volume occupied by the liquid metal would lead to deformation and relative separation of the grains of final amplitude equal to the liquid layer thickness.

In order to give an answer to this ongoing controversy, one has to characterize simultaneously the presence of nanometric penetration layers and possible associated relative grain movements of the same amplitude. These stringent requirements are fulfilled by a recently emerging variant of x-ray projection microscopy based on a Kirkpatrick-Baez (KB) focusing device [14]. Producing a secondary source of 90×90 nm^2, this technique allows one to perform this type of *in situ* measurement in the bulk of millimeter sized Al samples. The present investigation deals with one of the very first applications of such a microscope, currently under commission at the ID19 beam line of the European Synchrotron Radiation Facility (ESRF, France). The Ga layer thickness is deduced from x-ray absorption measurements. Very thin Ga films of about 5 nm thickness can be measured when setting the GB close to edge-on configuration [6]. In addition, relative grain movements can be determined to subpixel accuracy (i.e., about 10 nm) by image correlation techniques.

Experimental technique.—A pair of curved mirrors set in the KB geometry focuses [14] the beam to yield a secondary source of size 90×90 nm^2 with typical divergences γ of the order of a few milliradians. A multilayer coating on the first mirror selects a fixed x-ray energy (i.e., 20.5 keV). The curvature and the inclination of both mirrors are adjusted in such a way that the geometric aberrations are minimized and both focal planes are identical. This geometric magnification allows one to overcome the current limit of about 1 μm spatial resolution for microradiography in parallel beam geometry, which is connected to the finite impulse response of state-of-the-art detector systems [15]. Therefore, in the magnifying setup the ultimate resolution limit is no longer determined by the detector system but rather by the secondary source size. The sample is positioned in the divergent beam 78 mm downstream of this source. Set at a distance of 4 m, the detector records a 52 times magnified x-ray image (effective pixel size = 140 nm) with conspicuous Fresnel diffraction features. The temperature of the $10 \times 4 \times 0.8$ mm^3 bicrystal specimen is controlled in order to trigger the GBP process ($T_m = 29.8\,^\circ$C for Ga).

The relative movements between different sample regions are determined by image correlation techniques. The relative position shift of each region of interest (ROI) is deduced between two successive images and the temporal evolution is calculated from the cumulative difference of the position shifts between different regions. The precision by which the relative position of the ROI can be determined by image correlation methods is closely related to the signal-to-noise ratio and the spatial and temporal stability of the image contrast in the ROIs. In order to obtain subpixel accuracy, temporal drifts in the profile of the incoming beam and image distortions caused by residual errors in the shape profile of the reflecting mirror surfaces have to be corrected for. The spatial distortions have been determined from an image of a periodic reference object (2D grid) taken right after the Ga penetration experiment. The corresponding corrections are applied to the whole image series (i.e., 1000 frames) prior to further processing. Detailed sample preparation can be found in Ref. [6].

Results.—In Figs. 1(a)–1(d), four radiographs show the Ga penetration along a 150° symmetrical tilt around the ⟨110⟩ Al bicrystal (0.8 mm thick). Note that the observed width of the liquid layer is related to the geometrical projection of the GB and does not directly correspond to the real Ga film thickness [6]. Residual surface defects left over from the chemical etching (and subsequent polishing) are randomly distributed over the whole sample surface and can be clearly revealed by this inherently phase sensitive imaging technique. The contrast of these stains will allow the extraction of further information on the grain separation by image correlation techniques. By defining the time of arrival of the penetration front at the level of a given ROI [see Fig. 1(d)] as the moment when the mean Ga layer thickness in this ROI exceeds a certain threshold value (10 nm), it is possible to determine the position of the Ga front along the GB versus time, and hence its propagation rate. Figure 1(e) shows the penetrated distance versus time: a linear dependence corresponding to a propagation rate of 3.4 $\mu\mathrm{m}\cdot\mathrm{s}^{-1}$ is observed, in agreement with previous work [5,6].

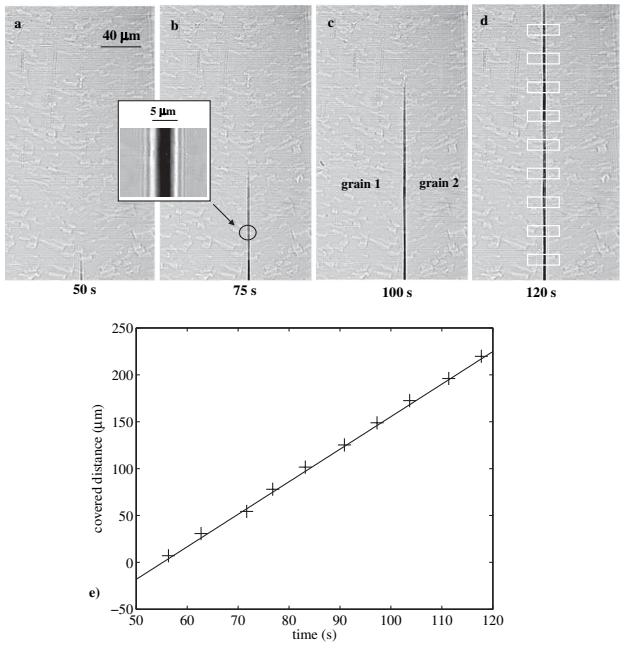

FIG. 1. (a)–(d) Microradiographs showing liquid Ga penetration along an Al bicrystal grain boundary. The inset shows the Fresnel interference pattern revealed by this inherently phase sensitive imaging technique. The last image (d) presents the ROIs studied. (e) Plot of the penetration distance versus time: a linear propagation rate of 3.4 $\mu\mathrm{m}\cdot\mathrm{s}^{-1}$ is found. The experimental uncertainty is represented by the crossed error bars.

In order to analyze the relative displacement between the two grains, three ROIs are chosen on both sides of the GB [Fig. 2(a)]. The relative displacement between the different ROIs is reported in Fig. 2(b). As expected, the movement between ROI 1 and ROI 2 on the same grain (δ_{12}) is nearly constant and close to zero. The small observed drift of about 5 nm can stem from a focus drift due to temperature variations of the x-ray optics or from a small sample rotation around the vertical axis [16]. The relative displacements δ_{13} and δ_{23} between grains clearly increase in the same way and amplitude during the penetration process. The time at which the Ga reaches the ROI level has been set to zero. The Ga layer thickness, w_{Ga}, determined from absorption is also plotted. Good agreement exists between the amplitude of the final relative displacement and the final thickness of the liquid film. However, one has to note the existence of a time interval between the onset of displacement, appearing first, and the arrival of the Ga penetration front. Similar observations have been found for three identical samples extracted from the same Al bicrystal ingot. Note that the observed relative movement cannot be attributed to rigid body movements of the entire, individual grains since the Ga penetration front has not yet reached the extremity of the GB.

Such relative displacements necessarily imply elastic and/or plastic deformation of the sample while it is not subject to any applied external stress. Let us assume that some level of stress normal to the GB plane exists (its origin will be discussed below). This situation is similar to the case of crack propagation under mode I loading in a single edge notched specimen treated in fracture mechanics [17]. Interpreted in this framework, the measured displacement of the ROIs would correspond to the *elastoplastic* displacement field in the direction normal to the crack plane (i.e., normal to the GB). Under the exclusive action of a tensile stress, the elastic contribution of the displacement of a point P positioned at a distance r from the crack tip, $V(r, \theta)$, is given by [17]

$$V(r,\theta) = \frac{1+\nu}{E} K_I \sqrt{\frac{2r}{\pi}} \sin(\theta/2)[2(1-\nu) + \cos^2(\theta/2)], \tag{1}$$

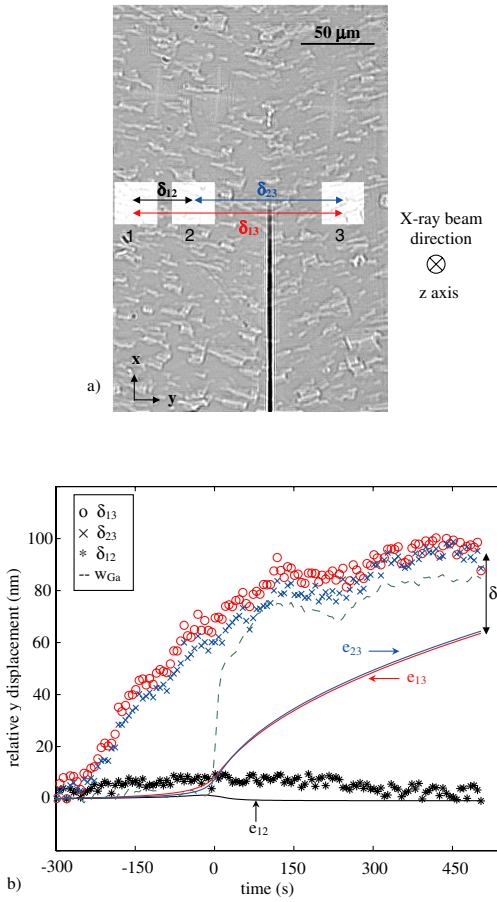

FIG. 2 (color online). (a) The three ROIs and relative distances studied (δ_{12}, δ_{13}, δ_{23}) during the penetration process. (b) Experimental evolution of the relative grain displacement with time (experimental uncertainty $\delta \pm 10$ nm not shown for the sake of clarity). A clear deformation of the grains is evidenced. The measured Ga thickness $w_{\mathrm{Ga}}(t)$ and the displacement that will be provoked by a purely elastic crack propagation (solid lines, e_{12}, e_{13}, e_{23}) with constant stress intensity factor $K_I = 0.045$ MPa $\cdot$ m$^{1/2}$ are also presented. The time at which the Ga reaches the ROIs has been set to zero (it corresponds to a penetrated GB length of about $a = 1.5$ mm).

where ν and E are the Poisson ratio and the Young's modulus of the solid, respectively, and θ is the polar angle. K_I is the stress intensity factor [17], which can roughly be estimated for small crack lengths (discussed below) as

$$K_I \approx \sigma_{yy}\sqrt{\pi a}, \tag{2}$$

where a is the crack length and σ_{yy} is the long range tensile stress. Note that for $\theta = \pm 180°$, one obtains directly the shape of the crack lips.

Considering the slope of the profile being well described with a stress intensity factor of $K_I = 0.045$ MPa $\cdot$ m$^{1/2}$, one gets from Eq. (1) the elastic contribution shown in Fig. 2(b) as solid lines (e_{12}, e_{13}, e_{23}). K_I was chosen as the fitting parameter to adjust the computed curves to the experimental ones *after* passage of the penetration front (i.e., for $t > 0$). For this K_I value, a plastic zone (PZ) is formed in front of the crack tip and it will extend along the GB with the crack [Fig. 3(a)]. The ROIs will thus also be displaced by the plastic deformation before the crack tip has actually reached them [Figs. 3(a) and 3(b)]. The extension of the plastic zone L_{PZ} can be estimated [17] as

$$L_{\mathrm{PZ}} = \frac{1}{2\pi}\left(\frac{K_I}{\sigma_{\mathrm{yield}}}\right)^2, \tag{3}$$

where σ_{yield} is the yield stress of the material. We can expect that the total plastic displacement contribution will be about equal to the so-called crack tip opening displacement [17], δ_{CTOD}, given by

$$\delta_{\mathrm{CTOD}} = \frac{2(1-\nu^2)}{1+\pi/2}\frac{K_I^2}{E\sigma_{\mathrm{yield}}}. \tag{4}$$

For the values of $K_I = 0.045$ MPa $\cdot$ m$^{1/2}$ and $\sigma_{\mathrm{yield}} = 0.8$ MPa, one obtains a plastic zone that extends over $L_{\mathrm{PZ}} = 500$ μm and $\delta_{\mathrm{CTOD}} = 25$ nm. This plastic contribution explains (1) the early separation of the ROIs observed ($\Delta t = L_{\mathrm{PZ}}/\dot{x} = 147$ s) and (2) the difference between the final measured displacement amplitude and

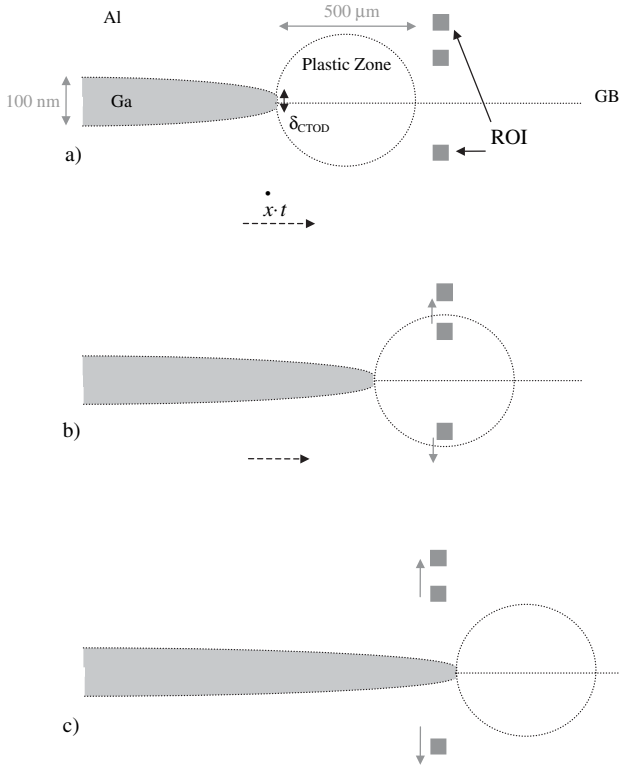

FIG. 3. Schematic view of the bulk point displacement by an elastoplastic crack propagating along the grain boundary: (a) before reaching the ROIs (no displacement), (b) the ROIs displaced by the plastic zone, and (c) after the passage of the plastic zone, the ROIs displaced by the elastic opening of the crack filled by liquid Ga plus the plastic contribution (crack tip opening displacement δ_{CTOD}).

the calculated elastic contribution using Eq. (1) [see Fig. 2(b)]. The Ga layer thickness corresponds to the sum of the elastic contribution and the plastic one, equal to the δ_{CTOD} value at the crack tip. Indeed, $w_{\mathrm{Ga}}(t)$ exhibits a rather abrupt increase at the beginning of the Ga layer detection, a behavior rather consistent with plastic blunting events.

Modeling GBP as a crack propagation process is certainly a simplified vision of the phenomenon, but it allows an understanding of the final amplitudes of both grain separation and Ga layer thickness. Moreover, since the Ga propagation is linear [Fig. 1(e)] and by expressing the total crack length as $a = x_0 + \dot{x}t$, one can write the elastic contribution w_{elastic} (with $\theta = 180°$) as

$$w_{\mathrm{elastic}}(a, t) \approx \frac{4\sqrt{2}(1 - \nu^2)}{E}\sigma\sqrt{(x_0 + \dot{x}t)\dot{x}t}. \qquad (5)$$

Consequently, the expected time dependence of the Ga layer thickness changes progressively from square root to linear thickening kinetics before Ga reaches the GB's extremity (in good agreement with Ref. [6]).

However, when considering the standard case of a sample submitted to a remote stress, the K_I expression contains a correction factor which accounts for the finiteness of the sample [18]. When this correction is applied, K_I and consequently the displacement are expected to increase by 1 order of magnitude when the crack length becomes comparable to the GB length, a fact in total disagreement with the experimental data. Actually, the results appear to be well described by a constant K_I value independent of the crack length all along the penetration process, giving support for a ''local driving mechanism'' at the crack tip, which would be consistent with the observed uniform linear crack propagation rate [5,6,16].

Regarding the possible origin of the stress, one has to remain rather speculative. The low values of the equivalent stress to consider (inducing a K_I of about 0.05 MPa $\cdot$ m$^{1/2}$) may be generated by a variety of interacting mechanical processes. Among them, one can think on the following: (1) torque terms of the surface tension balance at the crack tip, (2) an osmotic pressure in the liquid phase, or (3) residual stresses due to temperature gradient required for the growth of the Al bicrystal by using the Bridgman technique. Such stresses would have a tensile component and the same behavior all along the GB (again compatible with the constant penetration rate [5,6,16]).

X-ray projection microscopy based on a KB focusing device has proven to be a state-of-the-art nanoscale imaging technique with potential applications in today's materials science research. Simultaneous x-ray absorption and image correlation measurements of GBP by liquid Ga in Al bicrystals give direct evidence for nanometric grain deformation of same amplitude as the final Ga layer thickness. The profile of the penetration layers can be readily understood as the elastoplastic response of the material subject to weak levels of tensile stresses. This demonstrates that GBP in Al/Ga proceeds by an ''invasionlike'' rather than a ''replacementlike'' process. Taking into account this fundamental result should help to establish a consistent picture of the physical mechanisms involved and close the gap between the atomistic [4,19] and the microscopic knowledge of LME.

We would like to thank K. Wolski and M. Biscondi (EMSE, France) for providing the bicrystal samples as well as P. Bernard and R. Mokso (ESRF) for their help in experiment design and data analysis. We further acknowledge fruitful discussions with J. Baruchel, K. Wolski, F. Louchet, E. Glickman, and Y. Brechet.

*Corresponding author.
Electronic address: wolfgang.ludwig@insa-lyon.fr

[1] P. J. L. Fernandes, R. E. Clegg, and D. R. H. Jones, Eng. Fail. Anal. **1**, 51 (1994).
[2] P. J. L. Fernandes and D. R. H. Jones, Int. Mater. Rev. **42**, 251 (1997).
[3] G. Duscher, M. F. Chisholm, U. Alber, and M. Rühle, Nat. Mater. **3**, 621 (2004).
[4] D. I. Thomson, V. Heine, M. C. Payne, N. Marzari, and M. W. Finnis, Acta Mater. **48**, 3623 (2000).
[5] R. C. Hugo and R. G. Hoagland, Scr. Mater. **38**, 523 (1998).
[6] W. Ludwig, E. Pereiro-López, and D. Bellet, Acta Mater. **53**, 151 (2005).
[7] E. Pereiro-López, W. Ludwig, and D. Bellet, Acta Mater. **52**, 321 (2004).
[8] E. Rabkin, Scr. Mater. **39**, 685 (1998).
[9] D. Chatain, E. Rabkin, J. Derenne, and J. Bernardini, Acta Mater. **49**, 1123 (2001).
[10] W. M. Robertson, Trans. Metall. Soc. AIME **236**, 1478 (1966).
[11] E. E. Glickman, in *Multiscale Phenomena in Plasticity*, edited by J. Lépinoux *et al.* (Kluwer Academic, Dordecht, The Netherlands, 2000), p. 383.
[12] E. E. Glickman, Interface Sci. **11**, 451 (2003).
[13] A. Vilenkin, in *Diffusion, Segregation and Stresses in Materials*, edited by B. S. Bokstein and B. B. Straumal (Scitec, Uetikon-Zürich, Switzerland, 2003).
[14] O. Hignette, P. Cloetens, G. Rostaing, P. Bernard, and C. Morawe Rev. Sci. Instrum. **76**, 063709 (2005).
[15] A. Koch, C. Raven, P. Spanne, and A. Snigiriev, J. Opt. Soc. Am. A **15**, 1940 (1998).
[16] E. Pereiro-López, Ph.D. thesis, Institut National Polytechnique de Grenoble, France, 2004.
[17] H. Leibowitz, *Fracture, an Advance Treatise* (Academic Press, New York, 1968).
[18] *ASM Handbook: Fatigue and Fracture* (ASM International, Metals Park, Ohio, 1996), Vol. 19.
[19] R. Stumpf and P. J. Feibelman, Phys. Rev. **54**, 5145 (1996).